Bull. Mater. Sci., Vol. 39, No. 7, December 2016, pp. 1861–1870. © Indian Academy of Sciences.
DOI 10.1007/s12034-016-1322-8

First-principle studies of the ternary palladates $CaPd_3O_4$ and $SrPd_3O_4$

AMIN KHAN[1,2], ZAHID ALI[1,2,*], IMAD KHAN[1,2], SAEID JALALI ASADABADI[3] and IFTIKHAR AHMAD[1,2]

[1]Center for Computational Materials Science, University of Malakand, Chakdara, Dir (Lower) 18800, Pakistan
[2]Department of Physics, University of Malakand, Chakdara, Dir (Lower) 18800, Pakistan
[3]Department of Physics, Faculty of Science, University of Isfahan, Hezar Gerib Avenue, Isfahan 81744, Iran

MS received 12 August 2015; accepted 26 April 2016

Abstract. **Ternary palladates $CaPd_3O_4$ and $SrPd_3O_4$ have been studied theoretically using density functional theory approach. The calculated structural properties are consistent with the experimental findings. Mechanical properties show that these compounds are elastically stable, anisotropic and ductile in nature. The electronic properties reveal that they are narrow band gap semiconductors with band gaps 0.12 and 0.10 eV, correspondingly. Both materials are optically active in the infrared ranges of the electromagnetic spectrum. Narrow band gap semiconductors are efficient thermoelectric (TE) materials; therefore, TE properties are also studied and discussed. Furthermore, DFT and post-DFT calculations confirm the paramagnetic nature of these compounds.**

Keywords. **Ternary palladates; cohesive energy; elastic properties; *ab-initio* calculations; optical properties; thermoelectric properties.**

1. Introduction

Thermoelectric (TE) materials have attracted enormous attention during the last two decades due to the wide range of applications in advance technologies [1]. A TE device generates voltage when temperature gradient is applied across its ends. Single-crystalline solid material plays an effective role in practical applications of high-quality TE materials. The developments of new crystal growth techniques are important for the practical use as well as for the theoretical analysis of TE materials [2].

Alkaline earth palladates such as $CaPd_3O_4$ and $SrPd_3O_4$ have widespread applications in catalysis of organic reactions. Both the compounds are isostructural and narrow band gap semiconductors. However, isovalent ion substitution makes $CaPd_3O_4$ a good TE material [3,4]. The substitution of sodium (Na) by Sr in $SrPd_3O_4$ may enhance the figure of merit [4]. $CaPd_3O_4$ is a good candidate for being an excitonic insulator and used in switching and sensing devices [5].

Cahen *et al* [6] characterized single crystals of the ternary palladates $CaPd_3O_4$ and $SrPd_3O_4$ for the first time by scanning electron microscopy (SEM). Ichikawa and Terasaki [7] pointed out that the band gaps of these compounds are extremely small. $SrPd_3O_4$ and $CaPd_3O_4$ crystallize in space group Pm-3n (No. 223) with lattice constants 5.81 and 5.73 Å, respectively [8].

Wnuk *et al* [9] presented a chemical analysis of the $CaPd_3O_4$ material very clearly; the material possesses 9.24% Ca and 75.76% Pd, while the actual formula corresponds to 9.47% Ca and 75.41% Pd. Both materials exhibit semiconductor nature at room temperature, having resistivity on the order of 0.1 Ω cm [3,4,10]. The resistivity of $CaPd_3O_4$ decreases as temperature rises and the TE effect shows that the carriers are holes [9]. The electrical resistivity curve of $CaPd_3O_4$ is quite anomalous due to 4d transition metal and shows that resistivity is temperature dependent [5]. $CaPd_3O_4$ and $SrPd_3O_4$ are stabilized in Pd(II) oxidation state [11]. Muller and Roy [12] also experimentally reported the crystal structures of these compounds.

In this work we explore the theoretical aspects to clarify the electronic structure of the ternary palladates $CaPd_3O_4$ and $SrPd_3O_4$ for the emerging technological applications. All the calculations are performed using GGA, GGA + U and improved-mBJ techniques to investigate the structural, mechanical, electronic and magneto-optic properties of these compounds. Furthermore, the semi-classical post-DFT BoltzTraP code is utilized to study the TE properties of these compounds.

2. Computational details

All these calculations are performed using the full-potential linearized augmented plane waves (FPLAPWs) method [13] implemented in the WIEN2k code [14] within the framework of DFT. The Perdew–Burke–Ernzerhof [16] generalized gradient approximation (GGA) [15] is used for the calculations of the structural properties. Self-interaction corrections (SICs) GGA + U and improved-mBJ exchange potential are used for the calculations of the electronic

*Author for correspondence (zahidf82@gmail.com)

properties of these compounds [17,18]. In order to treat the Pd-d state properly we used $U = 2$ eV. The muffin-tin sphere radii are 2.27 a.u. for Ca, 1.99 a.u. for Pd and 1.71 a.u. for O in $CaPd_3O_4$, and 2.30 a.u. for Sr, 2.02 a.u. for Pd and 1.74 a.u. for O in $SrPd_3O_4$. For wave function in the interstitial region the plane wave cut-off value of $K_{max} = 7/R_{MT}$ is taken while the charge density is Fourier expanded up to $G_{max} = 14$ Ry. The energy convergence is taken during self-consistency cycles, while keeping the k points equal to 2300 for the full Brillouin zone integration [19].

Cubic-elastic software is utilized [20] to investigate the mechanical properties of these compounds. TE properties are calculated using post-DFT treatment using the BoltzTraP package [21].

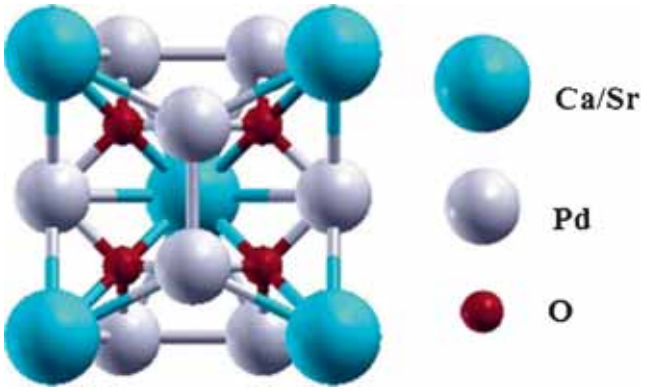

Figure 1. Unit cell crystal structure of the cubic Ca/$SrPd_3O_4$ with space group Pm-3n (No. 223).

3. Results and discussion

3.1 *Structural properties*

Alkaline-earth ternary palladates $CaPd_3O_4$ and $SrPd_3O_4$ compounds exist in cubic structure with lattice parameters 5.7471 and 5.826 Å, respectively, occurring in a space group Pm3n (No. 223) [5,8] as shown in figure 1. Structural optimization of each unit cell is performed using the Perdew–Burke–Ernzerhof generalized gradient approximation (GGA PBE-sol) scheme. Birch–Murnaghan [22] fitted equation of state is utilized to draw a relation between the energy and volume as shown in figure 2. The relaxed lattice constants for both compounds are evaluated at optimum volumes and compared to experimental results in table 1. The comparison with the experimental results shows that the calculated lattice constants of $CaPd_3O_4$ and $SrPd_3O_4$ are underestimated by 0.121 and 0.183%, respectively [12,23]. This underestimation is due to the famous GGA exchange-correlation effect. The small difference shows that our results are logical and reliable.

Bond lengths between the different atoms of these compounds are also calculated and presented in table 1. In $CaPd_3O_4$ palladium atoms are bonded with neighbouring four coplanar oxygen atoms; the calculated distance (Pd–O) is 2.029 Å, whereas the experimental bond distance between palladium and oxygen atom is 2.031 Å [23], which shows that our results are close to the experimental value. The bond length of Ca–Pd is 3.208 Å, Ca–O is 2.485 Å and Pd–O is 2.029 Å in $CaPd_3O_4$, whereas the bond lengths of Sr–Pd is 3.250 Å, Sr–O is 2.518 Å and Pd–O 2.056 Å for $SrPd_3O_4$.

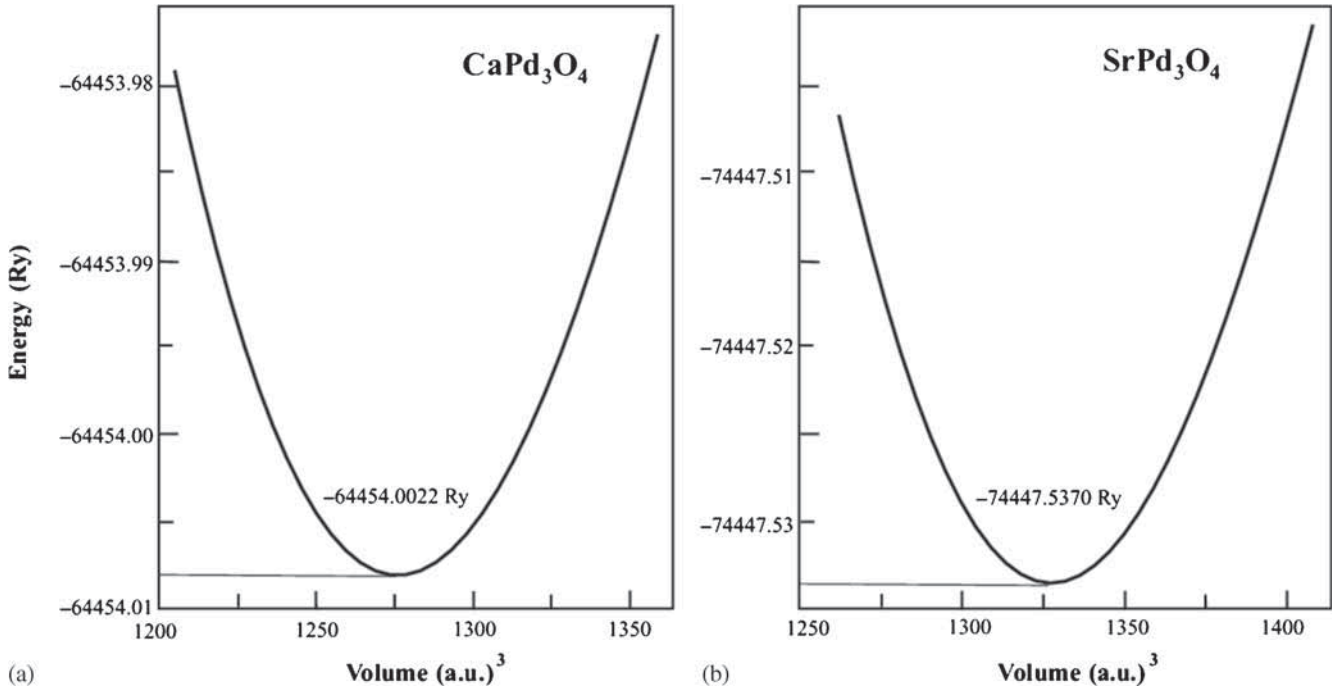

Figure 2. Variation of total energy *vs*. unit cell volume: **(a)** $CaPd_3O_4$ and **(b)** $SrPd_3O_4$.

Table 1. Calculated and experimental structural parameters like lattice constant (a_0), volume (V_0), ground state energy (E_0), bulk modulus (B) and bond lengths, cohesive energies (E_{coh}) and density (ρ) for $CaPd_3O_4$ and $SrPd_3O_4$.

Compound	Present	Experiment	Difference (%)
$CaPd_3O_4$			
a_0 (Å)	5.7424	5.7471[a], 5.7356[b], 5.747[c]	0.081
V_0 (Å)^3	189.35	188.68[b], 189[d], 189.822[a]	
E_0 (Ry)	−64454.0		
E_{coh} (eV)	−97.0780		
Band gap (eV)	0.12	0.12[e]	
Bond length (Å)			
Ca–Pd	3.2082	3.2063[b]	
Ca–O	2.4850	2.523[c], 2.4836[b], 2.49[d]	
Pd–O	2.0290	2.032[c], 2.0278[b], 2.03[d]	
$SrPd_3O_4$			
a_0 (Å)	5.8153	5.826[c], 5.8120[b]	0.183
V_0 (Å)^3	196.66	196.33[b]	
E_0 (Ry)	−74447.5		
E_{coh} (eV)	−96.5980		
Bandgap (eV)	0.10		
Bond length (Å)			
Sr–Pd	3.2508	3.2490[b]	
Sr–O	2.5181	2.488[c], 2.5167[b]	
Pd–O	2.0560	2.0523[a], 2.0549[b], 2.059[c]	

[a]Ref. [23], [b]Ref. [8], [c]Ref. [12], [d]Ref. [9], [e]Ref. [5].

These bond lengths have unique importance as they can be used to calculate the tolerance factor of a compound and crystal structure can be guessed.

3.2 *Cohesive energy*

Cohesive energy plays an important role in the formation of a material and defines the stability of a compound. Cohesive energy is the energy difference between the bulk materials at equilibrium and the free atoms in their ground state [24,25]. The crystal cohesive energy (CCE) is important in solid state theory and microscopic calculations of pure elements and ionic compounds. The calculation for the CCE of ionic compound is based on classical Coulomb interaction and depends on the atomic size [26].

To discuss the stability of $CaPd_3O_4$ and $SrPd_3O_4$ compounds, the cohesive energies of these compounds are calculated by the well-known expression [27]

$$E_{coh} = E_{APd_3O_4} - (2E_A + 6E_{Pd} + 8E_O). \quad (1)$$

In equation (1) $E_{APd_3O_4}$ represents the cell energy of $CaPd_3O_4$ and $SrPd_3O_4$; E_A and E_O are the free energies of Ca/Sr and O, respectively, obtained by GGA calculations. The calculated cohesive energies are −97.078 and −96.598 eV for $CaPd_3O_4$ and $SrPd_3O_4$, respectively, which are tabulated in table 1. The table shows that the cohesive energy of $CaPd_3O_4$ is more than the cohesive energy of $SrPd_3O_4\{-E_{coh}\,(CaPd_3O_4) > -E_{coh}\,(SrPd_3O_4)\}$; hence $CaPd_3O_4$ is a more strongly bound system than $SrPd_3O_4$ material.

3.3 *Mechanical properties*

Elastic constants determine the response of a crystal to external force, as characterized by bulk modulus (B_0), shear modulus (G) and Young's modulus (Y) as well as the Poison's ratio (ν). These parameters clearly determine the strength as well as the stability of materials using the relations of elastic constants [28,29]: Viogot shear modulus (G_v) corresponding to the upper bound of G values and Reuss's shear (G_R) modulus for the cubic crystal corresponding to the lower bound values. To the best of our knowledge there is no experimental or theoretical data available on the elastic constants of these compounds in literature.

Elastic constant values are obtained using numerical calculations of these compounds by computing the stress tensor using the recently developed method implanted in the WIEN2k code [20]. The three independent elastic constants C_{11}, C_{12} and C_{44} for $CaPd_3O_4$ are 295.60, 127.62 and 75.83 GPa, whereas for $SrPd_3O_4$ they are 276.10, 127.29 and 88.47 GPa, respectively. The mechanical stability in cubic symmetry must obey the restrictions C_{11}–$C_{12} > 0$, $C_{44} > 0$, $C_{11} + 2C_{12} > 0$ [30] and also $C_{12} < C_{11}$. Our calculated elastic constants follow these cubic stability conditions; for

instance $C_{12} < B < C_{11}$ [31], which reveal that these compounds are stable against elastic deformations.

Sound velocities for longitudinal and shear waves (V_L and V_S) and sound average velocity (V_m) are calculated using bulk modulus (B), isotropic shear modulus (G) and mass density (ρ) [32] and are listed in table 2. The average sound velocity gives explicit information about lattice vibrations [33]. Our calculated longitudinal sound velocities for $CaPd_3O_4$ and $SrPd_3O_4$ are 5486.69 and 6006.70 m s^{-1}, shear sound velocities are 2720.31 and 3221.71 m s^{-1} and mean sound velocities are 3053.18 and 3597.70 m s^{-1}, respectively. From these calculations it is clear that $SrPd_3O_4$ has higher sound velocities than $CaPd_3O_4$.

Debye temperature (θ_D) is one of the most important parameters and it determines the thermal characteristics of a material, atomic vibration and theories relating phonons [34]. The Debye temperature is determined by the empirical formula [32]

$$\theta_D = \left[\left(\frac{\hbar}{K_B}\right)\left(\frac{3n}{4\pi}\right)\left(\frac{N_A\rho}{M}\right)\right]^{1/3} V_m, \quad (2)$$

where n is the number of atoms, $\hbar$ the Planck constant, N_A Avogadro's number, ρ mass density, M molecular weight in the molecule and K_B the Boltzmann constant. The calculated densities and Debye temperatures for both compounds $CaPd_3O_4$ and $SrPd_3O_4$ are 7.426 and 7.953 g cm^{-3}, 251.33 and 292.44 K, respectively. To the best of our knowledge, no information about the densities and Debye temperatures is available for $CaPd_3O_4$ and $SrPd_3O_4$; hence, these theoretical results can be reliable for further experimental and theoretical studies.

Table 2. Calculated elastic moduli C_{ij}, bulk modulus (B), Young's modulus (Y), Voigt's shear modulus (G_v), Reuss's shear modulus (G_R), isotropic shear modulus (G), B/G ratio, Poisson's ratio (υ), transverse and longitudinal sound velocity, average sound velocity (V_s, V_L and V_m), Debye temperature (θ_D), Lame's coefficients (λ and μ), Kleinman parameter (ζ) and anisotropy constant (A).

Parameter	$CaPd_3O_4$	$SrPd_3O_4$
C_{11} (GPa)	295.60	276.10
C_{12} (GPa)	127.62	127.29
C_{44} (GPa)	75.830	88.470
B (GPa)	150.28	176.89
Y (GPa)	156.74	214.97
G_v (GPa)	59.100	82.844
G_R (GPa)	50.810	82.250
G (GPa)	54.953	82.550
ρ (g cm^{-3})	7.426	7.953
B/G	1.8800	1.8450
υ	0.2730	0.2700
V_L (m s^{-1})	5486.69	6006.70
V_s (m s^{-1})	2720.31	3221.71
V_m (m s^{-1})	3053.18	3597.7
θ_D (K)	251.33	292.44
λ	19.670	20.320
μ	128.84	132.10
ζ	0.7250	0.7710
A	0.9020	1.1890

Kleinman is another important internal strain parameter (ζ) [35]; it explains the relative bond bending and bond stretching. For bond bending the Kleinman parameter is zero while for bond stretching its value is 1. The Kleinman parameter of $SrPd_3O_4$ is more than that of $CaPd_3O_4$ and ζ is close to 1 (shown in table 2), which confirms that the bond stretching in $SrPd_3O_4$ is more than in $CaPd_3O_4$.

The anisotropic factor (A) for a material measures the degree of elastic anisotropy and can be obtained from the three independent elastic constants [36]. For an ideal isotropic system the anisotropic factor is unity and deviation from unity measures the quantity of elastic anisotropy. From table 2, it is clear that the calculated anisotropic factors for $CaPd_3O_4$ and $SrPd_3O_4$ deviate from unity, which clarifies that these compounds are elastically anisotropic and the sound waves will travel with velocities in different directions.

The other interesting elastic parameters are Lame's constants (λ and μ), which depend on the material nature and temperature. Lame's constants are calculated from Young's modulus and Poisson's ratio [36]. These constants represent a parameterization of the elastic moduli for homogeneous isotropic media. The Lame's constants (table 2) confirm the anisotropy of these compounds by not satisfying the isotropic conditions, i.e., $\lambda = C_{12}$ and $\mu = C'$. Our calculated results of Lame's constants for $CaPd_3O_4$ compound are $\lambda = 19.67$, $\mu = 128.84$ and for $SrPd_3O_4$, $\lambda = 20.32$ and $\mu = 132.1$. $SrPd_3O_4$ shows dominancy as compared to $CaPd_3O_4$ in anisotropy, which reveals that $SrPd_3O_4$ is more anisotropic than $CaPd_3O_4$.

Pugh ratio (B/G) [37,38] is an index for the ductility and brittleness of a material. B/G ratio is greater than 1.75 for ductile material; otherwise the material is brittle. Our calculated values of B/G are greater than 1.75 for both the compounds shown in table 2, demonstrating the ductile nature of these compounds, and revealing that $CaPd_3O_4$ is more ductile than $SrPd_3O_4$. The Poisson ratio (ν) provides information about the bond nature. The Poisson ratio for covalent materials is on the order of 0.1, whereas for ionic compound $\nu = 0.25$ [39]. From our results $\nu \approx 0.273$ for $CaPd_3O_4$ and 0.270 for $SrPd_3O_4$, showing the high covalency in these compounds.

3.4 *Electronic properties*

Self-consistent field (SCF) calculations are performed using GGA + U and improved-mBJ to compute the electronic band structures of $CaPd_3O_4$ and $SrPd_3O_4$ and are shown in figure 3. It is obvious from figure 3 that a narrow gap exists between the valence and conduction bands for both the compounds at Γ symmetry points of the Brillouin zone. Hence, both the compounds are narrow bandgap semiconductors. The calculated band gap of $CaPd_3O_4$ by both potentials GGA + U and improved-mBJ is 0.12 eV while for $SrPd_3O_4$ the gap is 0.11 eV. The comparison of the calculated results

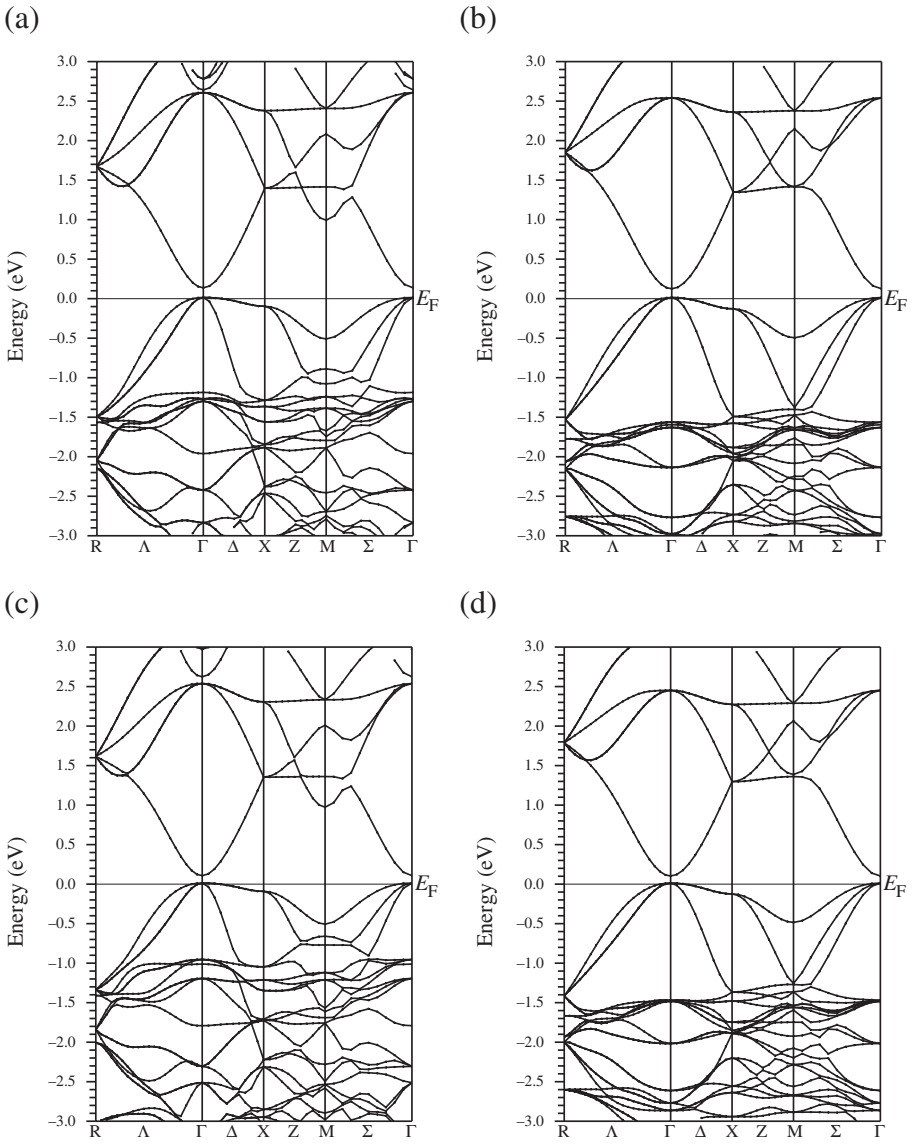

Figure 3. Electronic band structures: **(a**, **b)** $CaPd_3O_4$ and **(c**, **d)** $SrPd_3O_4$; (**a**, **c**) by GGA + U and (**b**, **d**) by improved mBJ.

of $CaPd_3O_4$ with experiments [5] shows close agreement, which demonstrates the reliability of our work.

To investigate the involvement of various states in the band structure, we present total and partial density of states in figures 4 and 5a and b, respectively. It can be observed from figure 4 that the spin-dependent band profiles for $CaPd_3O_4$ and $SrPd_3O_4$ are similar and symmetric with a slight difference in details. Figure 5a and b explains the main contributions of different states in which the major contributions in the VB for both compounds are due to O-p and Pd-d states occurring up to the Fermi level. The Pd-s, Pd-p and O-s states lie in the bottom of the VB and are not shown in the figures. In figure 5a and b the major contributions of Pd-d and O-p states start from −7.5 eV and reach the Fermi level for both compounds with a small difference in details with a smaller contribution in CB. The O-p state contains two peaks in VB for $CaPd_3O_4$: one peak occurs at energy −6.3 eV, while the other is at energy −1.4 eV. Similarly $SrPd_3O_4$ contains three peaks in VB at different energies levels, i.e., at 6.3, 4.8 and 1.8 eV, whereas Ca/Sr-d states occur in CB above 4 eV.

3.5 *Optical properties*

These materials are narrow direct band gap semiconductors, which are optically active; hence the optical nature of these compounds is also investigated. A suitable understanding of the optical properties of a compound is very important for the useful applications in photonics and optoelectronics [40]. As both the compounds have very similar band gaps, optical properties like dielectric functions $\varepsilon(\omega)$, refractive index $n(\omega)$, reflectivity $R(\omega)$, energy loss function $L(\omega)$ and

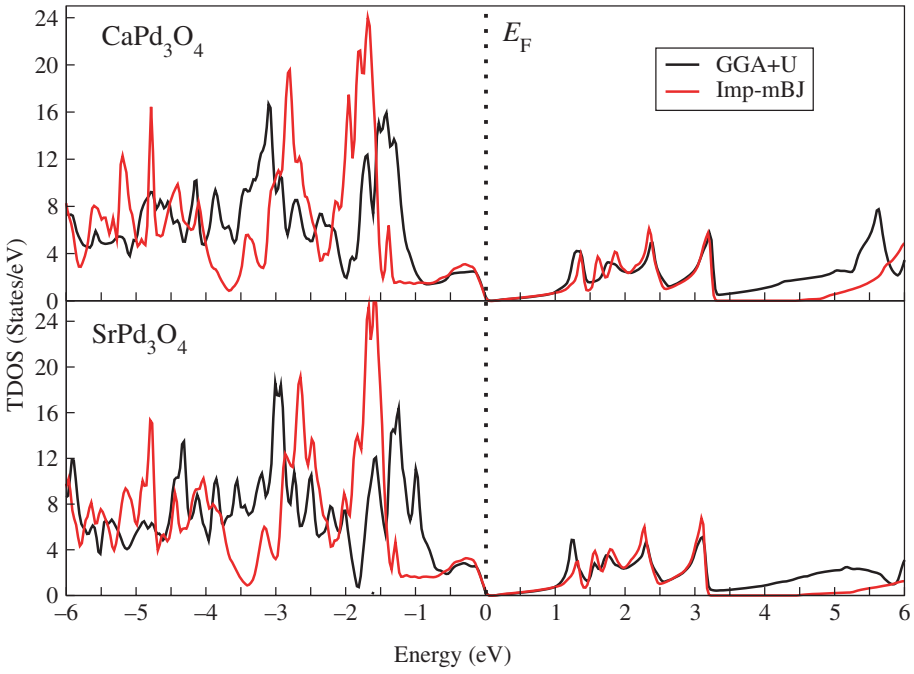

Figure 4. Total density of states by GGA + U and improved-mBJ of $CaPd_3O_4$ and $SrPd_3O_4$.

oscillator strength $\sigma(\omega)$ of only $CaPd_3O_4$ are calculated and shown in figure 6.

The polarizability of a material can be explained by the real part of dielectric function $\varepsilon_1(\omega)$ shown in figure 6a. The zero-frequency limit $\varepsilon_1(0)$ has a value of 7.28, which confirms that the compound is a high-dielectric-constant material. From the zero frequency limit $\varepsilon_1(0)$ it starts rising and becomes maximum at energy 1.59 eV; then from this highest value, it starts decreasing with some variations. These variations are due to interband transitions. The real part of dielectric function reaches the lowest value at 29.31 eV. The imaginary part of complex dielectric function is one of the most important optical parameters because it reflects optical gap as well as optical absorption. Figure 6b shows the imaginary part of dielectric function $\varepsilon_2(\omega)$ of $CaPd_3O_4$ in the energy range 0–45 eV. Figure 6b indicates that the significant peak for dielectric function is at approximately 0.016 eV. The plot also reveals that $CaPd_3O_4$ has tough absorbing capacity in the energy range 0.016–31.1 eV. Different peaks in this plot are due to different inter-band transitions found between the valence band and the conduction band. As these materials have narrow and direct band gap nature, they are capable runners for optoelectronic devices in the infrared range of electromagnetic spectrum.

The refractive index has inverse relation with the band gap, i.e., smaller the band gap of a semiconductor, larger the refractive index and *vice versa*. The refractive index of $CaPd_3O_4$, shown in figure 6c, decreases with increase in energy and at zero frequency the calculated refractive index is 2.74. The refractive index vanishes at energy 30.6 eV. The lower energy humps correspond to fundamental band gaps, whereas the peak points are related to inter-band transition.

The reflectivity $R(\omega)$ is plotted in figure 6d, which explains the surface behaviour of the material. To satisfy the zero-frequency limit of any materials the reflectivity is less than 3.18 at Γ symmetry point of the full Brillouin zone. It is obvious from the plot that the minimum reflectivity found in the energy range 0–27 eV is due to collective plasma resonance. There is a higher reflection peak observed at energy 30 eV.

To investigate various aspects of the materials, electron energy loss spectroscopy (EELS) is an essential tool [41]. It gives knowledge regarding elastically scattered and non-scattered electrons as well as information about the number and type of atoms being struck by the beam [42,43]. The EELS for $CaPd_3O_4$ is plotted in figure 6e. From the figure it is clear that at lower energies there is no scattering. Wavelengths outside the transparency region bring tough polarization, which causes dispersion in the refractive index and rise in the propagation loss. Inelastic scattering and maximum loss are observed in the intermediate energy range, where the maximum peaks are observed in the energy range of 31.05 eV.

The numbers of effective electrons involved in the optical transitions are calculated in terms of sum rule. The oscillator strength (sum rule) is a dimensionless quantity and reveals the strength of transitions from valence to conduction band and is presented in figure 6f. It rises gradually and reaches 27.62 eV having 47 numbers of effective electrons, and then there is another rise starting at energies around 27.62 eV. Finally, the oscillator strength saturates at 30.55 eV having 58 numbers of effective electrons for $CaPd_3O_4$. Similar properties are observed for $SrPd_3O_4$ with a small difference in details (plot not given). Hence both compounds are optically active in the infrared region of the electromagnetic spectrum.

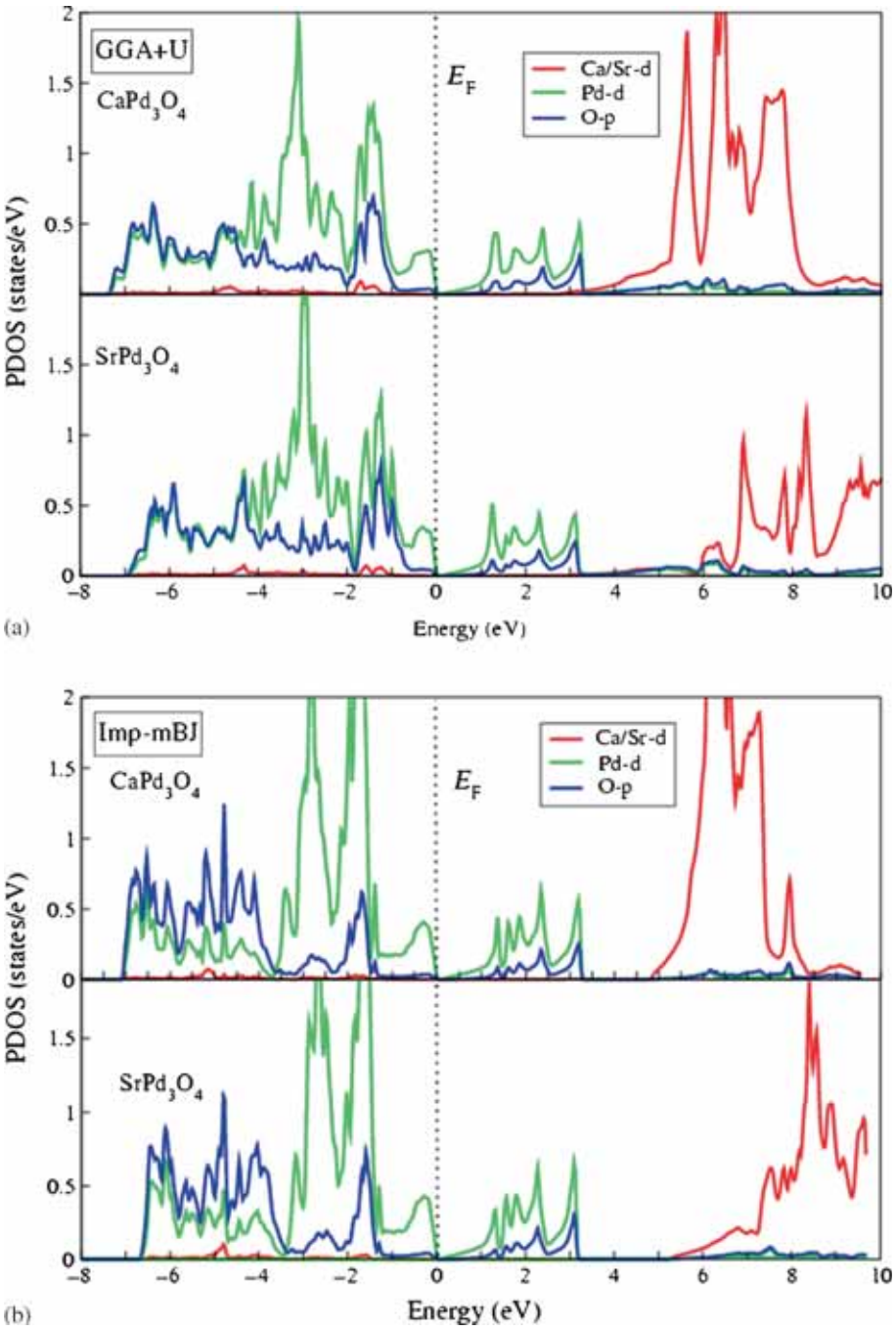

Figure 5. Partial density of states by **(a)** GGA + U and **(b)** improved-mBJ of $CaPd_3O_4$ and $SrPd_3O_4$.

3.6 *Thermoelectric properties*

Narrow band gap semiconductors are efficient TE materials. Keeping in view the importance of these materials the Seebeck coefficient is calculated for both compounds. The Seebeck coefficient is the most fundamental parameter to understand the TE behaviour of a compound as it estimates the fundamental electric parameter, i.e., voltage due to temperature [44]. Mathematically the Seebeck coefficient can be expressed as $S = \Delta V/\Delta T$, where ΔV is the TE voltage and ΔT is the temperature difference [45,46]. The Seebeck coefficient (S) gives a useful picture of the electronic structure of the material around the Fermi level [47]. As the Seebeck coefficient is moderate there should be a single-type carrier, and these low carriers lead to the semiconductor nature [48], which confirms the semiconducting nature of these materials.

The calculated Seebeck coefficients of $CaPd_3O_4$ and $SrPd_3O_4$ are presented in figure 7. It is obvious from the figure that the Seebeck coefficient increases with rising temperature. In case of $CaPd_3O_4$ the Seebeck coefficient obeys the

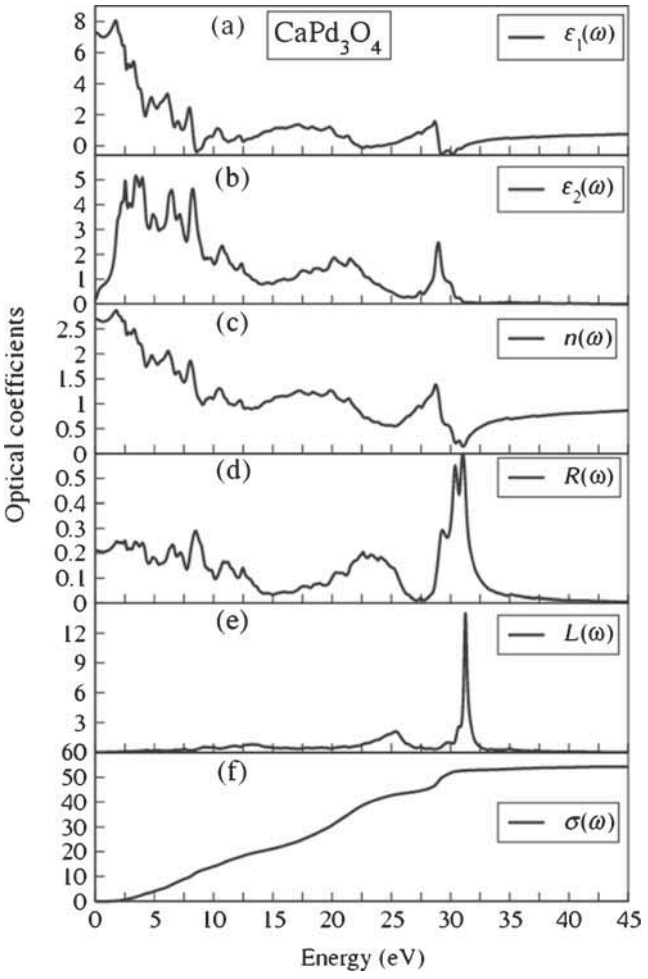

Figure 6. Optical parameters: **(a)** dielectric function, **(b)** absorption coefficient, **(c)** refractive index, **(d)** reflectivity, **(e)** energy loss function and **(f)** oscillator strength of $CaPd_3O_4$.

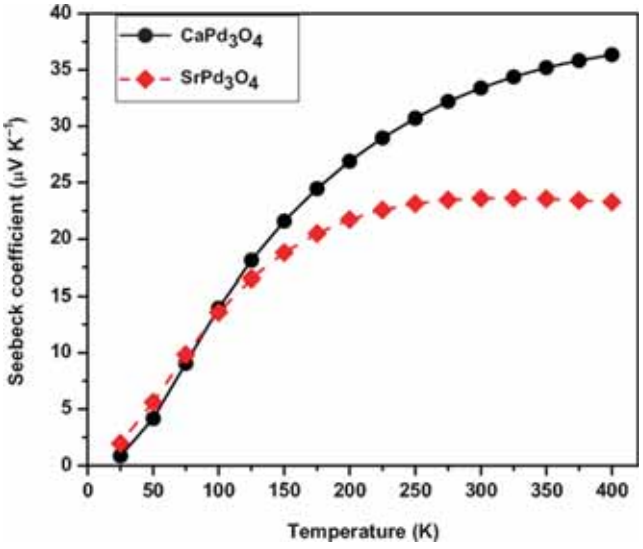

Figure 7. Seebeck coefficient (μV K^{-1}) *vs.* temperature (K) for $CaPd_3O_4$ and $SrPd_3O_4$.

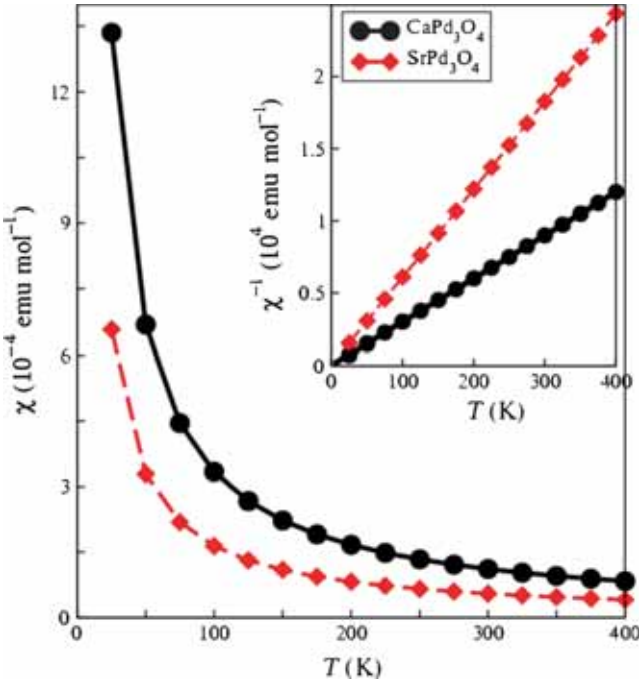

Figure 8. Magnetic susceptibility (χ) and its inverse *vs.* temperature (T) of $CaPd_3O_4$ and $SrPd_3O_4$.

experimental trend and reaches 37.0 μV K^{-1} at temperature 400 K [7]. For $SrPd_3O_4$ the Seebeck coefficient increases with rise in temperature up to 300 K; then it decreases with further increase in temperature and follows the experimental trend. Our theoretical results are consistent with the experimental results [4,49]. The calculated Seebeck coefficients for both the compounds are positive, which indicate that the majority carrier in both compounds are holes; hence we predict that these compounds could be used as good TE materials.

3.7 *Magnetic properties*

To know the magnetic nature of these compounds, optimizations are performed for paramagnetic phase (non-magnetic phase) as well as for ferromagnetic phase. These compounds lower their energies in paramagnetic phase; the energy difference between paramagnetic and ferromagnetic phase ($\Delta E = E_{PM}-E_{FM}$) is −0.0002 and −0.0047 Ry for $CaPd_3O_4$ and $SrPd_3O_4$, respectively. These energy differences show that these compounds are stable in the paramagnetic (non-magnetic) phase.

Magnetic susceptibility is one of the most important physical properties of the condensed matter; it specifies the behaviour of a material and phase transition with the change in temperature [50]. The temperature dependence of magnetic susceptibility (χ) is measured for $CaPd_3O_4$ and $SrPd_3O_4$ compounds as shown in figure 8. Comparison of the calculated χ results with the experimental data of Samata

et al [23] shows good agreement at 300 K. Magnetic susceptibility for both compounds has been calculated over the temperature range of 0–400 K. In the temperature range 200–400 K the calculated $\chi(T)$ is found to be almost linear. Hence both compounds are paramagnetic; the plots are consistent with Curie–Weiss law of paramagnetism [50].

The plot shows that magnetic susceptibility for $CaPd_3O_4$ is $13.0(10^{-4}$ emu $mol^{-1})$, whereas for $SrPd_3O_4$ it is $6.5(10^{-4}$ emu $mol^{-1})$ at temperature 25 K. From the plot it is clear that magnetic susceptibility dramatically falls up to temperature 250 K and then steadily decreases with increasing temperature. The magnetic susceptibility recorded is $1(10^{-4}$ emu $mol^{-1})$ for $CaPd_3O_4$ and $0.5(10^{-4}$ emu $mol^{-1})$ for $SrPd_3O_4$ at temperature 300 K. Our result shows that χ is small and positive, which demonstrate the paramagnetic behaviour, and this is confirmed by the inverse plot of χ *vs.* temperature. The magnetic susceptibility plots of both compounds are consistent with the experimental results [51,52]. The inverse plot of χ *vs.* T is consistent with the well-known Curie–Weiss law [53], where θ shows the Weiss temperature and for paramagnetic material $\theta = 0$. Hence our DFT as well as post-DFT calculations confirm that these compounds are paramagnetic in nature.

4. Conclusions

In summary, ternary palladates $CaPd_3O_4$ and $SrPd_3O_4$ are studied theoretically using GGA, GGA + U and improved-mBJ potentials in the framework of DFT. The calculated lattice constants for both compounds are very close to the experimental values. The cohesive energy shows that $CaPd_3O_4$ is more stable than $SrPd_3O_4$. Mechanical properties reveal higher covalent contribution in these compounds. The calculated B/G values are greater than 1.75, which confirms ductile nature of these compounds. The electronic properties reveal that $CaPd_3O_4$ and $SrPd_3O_4$ are narrows band gap semiconductors with values of 0.12 and 0.10 eV, respectively, at Γ symmetry points of the Brillouin zone. Both compounds are found to be optically active in the infrared range of electromagnetic spectrum. The calculated Seebeck coefficient reveals that these compounds are good candidates for thermoelectric devices. The stable magnetic phase of these palladates is optimized, which reveals that both materials are stable in paramagnetic phase. The post-DFT calculations of magnetic susceptibility confirm that these compounds are paramagnetic materials.

References

[1] Li J F, Liu W S, Zhao L D and Zhou M 2010 *NPG Asia Mater.* **2** 152

[2] Saramat A, Svensson G, Palmqvist A E C, Stiewe C, Mueller E, Platzek D *et al* 2006 *J. Appl. Phys.* **99** 023708

[3] Taniguchi T, Nagata Y, Ozawa T C, Sato M, Noro Y, Uchida T and Samata H 2004 *J. Alloys Compd.* **373** 67

[4] Ozawa T C, Matsushita A, Hidaka Y, Taniguchi T, Mizusaki S, Nagata Y *et al* 2008 *J. Alloys Compd.* **448** 77

[5] Hase I and Nishihara Y 2000 *Phys. Rev. B* **62** 13426

[6] Cahen D, Ibers J A and Shannoni R D 1972 *Inorg. Chem.* **11** 2311

[7] Ichikawa S and Terasaki I 2003 *Phys. Rev. B* **68** 233101

[8] Smallwood P L, Smith M D and Loye H C Z 2000 *J. Cryst. Growth* **216** 299

[9] Wnuk R C, Touw T R and Post B 1964 *J. Res. Dev.* **8** 185

[10] Itoh K and Tsuda N 1999 *Solid State Commun.* **109** 715

[11] Wang Y, Walker D, Chen B H and Scott B A 1999 *J. Alloys Compd.* **285** 98

[12] Muller O and Roy R 1971 *Adv. Chem.* **98** 28

[13] Singh D 1994 *Plane wave pseudo-potential and LAPW method* (Bosten, Dortrecht, London: Kluwer Academic Publishers)

[14] Blaha P, Schwarz K, Madsen G, Kvasnicka D and Luitz J 2014 *WIEN2k*: *an augmented plane waves plus local orbitals program for calculating crystal properties, WIEN2k 14.2* (Vienna, Austria: Institute of Physical and Theoretical Chemistry, Vienna University of Technology)

[15] Perdew J P, Burke K and Wang Y 1996 *Phys. Rev. B* **54** 16533

[16] Perdew J P, Burke S and Ernzerhof M 1996 *Phys. Rev. Lett.* **77** 3865

[17] Koller D, Tran F and Blaha P 2012 *Phys. Rev. B* **85** 155109

[18] Anisimov V I, Solovyev I V, Korotin M A, Czyzyk M T and Sawatzky G A 1993 *Phys. Rev. B* **48** 16929

[19] Kervan N 2012 *J. Magn. Magn. Mater.* **324** 4114

[20] Jamal M, Asadabadi S J, Ahmad I and Aliabad H A R 2014 *Comput. Mater. Sci.* **95** 592

[21] Madsen G K H and Singh D J 2006 *Comput. Phys. Commun.* **175** 67

[22] Murnaghan F D 1944 *Proc. Natl. Acad. Sci.* **30** 244

[23] Samata H, Tanaka S, Mizusaki S, Nagata Y, Ozawa T C, Sato A and Kosuda K 2012 *J. Crystallization Process Technol.* **2** 16

[24] Ali Z, Abdul Sattar A, Asadabadi S J and Ahmad I 2015 *J. Phys. Chem. Solids* **86** 114

[25] Gaudoin R, Foulkes W M C and Rajagopal G 2008 *J. Phys.*: *Condens. Matter* **14** 8787

[26] Li J P, Dong S L, Meng S H, Luo X G and Zhang Y M 2010 *Front. Mater. Sci. China* **4** 245

[27] Suetin D V, Annikov V V, Shein I R and Ivanovskii A L 2009 *Phys. Status Solidi B* **246** 1646

[28] Chen W and Jiang J Z 2010 *J. Alloys Compd.* **499** 243

[29] Singh R P, Singh R K and Rajagopalan M 2011 *Chalcogenide Lett.* **8** 325

[30] Sinko G and Vand S N A 2002 *J. Phys. Condens. Matter.* **14** 6989

[31] Khenata R, Bouhemadou A, Sahnoun M, Reshak A H, Baltache H and Rabah M 2006 *Comput. Math. Sci.* **38** 29

[32] Haddadi K, Bouhemadou A, Louail L, Maabed S and Maouche D 2009 *Phys. Lett. A* **373** 1777

[33] Belomestnykh V N 2004 *Tech. Phys. Lett.* **30** 91

[34] Ibrahim A M 1988 *Nucl. Instrum. Methods Phys. Res. B* **34** 135

[35] Kleinman L 1962 *Phys. Rev.* **128** 2614

[36] Gupta D C and Singh S K 2012 *J. Alloys Compd.* **515** 26

[37] Yuan P F and Ding Z J 2008 *Physica B* **403** 1996

[38] Pugh S F 1954 *Philos. Mag. Ser.* **45** 823

[39] Bouhemadou A, Khanate, Kharoubi M, Seddik T, Reshak A H and Douri Y A 2009 *Comput. Mater. Sci.* **45** 474

[40] Khan I, Subhan F, Ahmad I and Ali Z 2015 *J. Phys. Chem. Solids* **83** 75

[41] Loughin S, French R H, Noyer L K, Ching W Y and Xu Y N 1996 *J. Phys. D*: *Appl. Phys.* **29** 1740

[42] Aliabad H A R, Hosseini S M, Kompany A, Youssefi A and Kakhki E A 2009 *Phys. Status Solidi B* **246** 1072

[43] Egerton R F 2009 *Rep. Prog. Phys.* **72** 016502

[44] Park M S, Song J H, Medvedeva J E, Kim M, Kim I G and Freeman A J 2010 *Phys. Rev. B* **81** 155211

[45] Ramu A T, Cassels L E, Hackman N H, Lu H, Zide J M O and Bowers J E 2010 *J. Appl. Phys.* **107** 083707

[46] Sales B C, Mandrus D and Williams R K 1996 *Science* **272** 1325

[47] Xu B, Liang J, Li X, Sun J F and Yi L 2011 *Eur. Phys. J. B* **79** 275

[48] Snyder G J and Toberer E S 2008 *Nat. Mater.* **7** 105

[49] Shi X, Yang J, Salvador J R, Chi M, Cho J Y, Wang H *et al* 2011 *J. Am. Chem. Soc.* **133** 7837

[50] Nagamatsu J, Nakagawa N, Muranaka T, Zenitani Y and Akimitsu J 2001 *Nature* **410** 63

[51] Julien C M, Salah A A, Mauger A and Gendron F 2006 *Ionics* **12** 21

[52] Vekua T 2014 *Phys. Rev. B* **89** 121112(R)

[53] Kittel C 2004 *Introduction to solid state physics,* 8th edn (New York: Wiley)